Author Manuscript

Author Manuscript

Author Manuscript

Author Manuscript

HHS Public Access

Author manuscript

Clin Cancer Res. Author manuscript; available in PMC 2018 January 15.

Published in final edited form as:

Clin Cancer Res. 2017 January 15; 23(2): 536–548. doi:10.1158/1078-0432.CCR-16-0725.

Preclinical Benefit of Hypoxia-Activated Intraarterial Therapy with Evofosfamide in Liver Cancer

Rafael Duran, M.D.[1,2], **Sahar Mirpour, M.D.**[1], **Vasily Pekurovsky**[1], **Shanmugasundaram Ganapathy Kanniappan, Ph.D.**[1], **Cory F. Brayton, D.V.M.**[3], **Toby C. Cornish, M.D., Ph.D.**[4], **Boris Gorodetski**[1], **Juvenal Reyes, M.D.**[5], **Julius Chapiro, M.D.**[1,2], **Rüdiger E. Schernthaner, M.D.**[1,2], **Constantine Frangakis, Ph.D.**[6], **MingDe Lin, Ph.D.**[7], **Jessica D. Sun, Ph.D.**[8], **Charles P. Hart, Ph.D.**[8], and **Jean-François Geschwind, M.D.**[2]

[1] Russell H. Morgan Department of Radiology and Radiological Science, Division of Vascular and Interventional Radiology, The Johns Hopkins Hospital, Baltimore, MD.

[2] Department of Diagnostic Radiology and Imaging Science, Yale University School of Medicine, New Haven, CT.

[3] Department of Molecular and Comparative Pathobiology, The Johns Hopkins University School of Medicine, Baltimore, MD.

[4] Department of Pathology, Division of Gastrointestinal and Liver Pathology, The Johns Hopkins University School of Medicine, Baltimore, MD.

[5] Department of Radiation Oncology and Molecular Radiation Sciences, The Johns Hopkins Hospital, Baltimore, MD.

[6] Department of Biostatistics, The Johns Hopkins Bloomberg School of Public Health, Baltimore, MD.

[7] U/S Imaging and Interventions (UII), Philips Research North America, Briarcliff Manor, NY.

[8] Threshold Pharmaceuticals, South San Francisco, CA.

Abstract

Purpose—To evaluate safety and characterize anticancer efficacy of hepatic hypoxia-activated intraarterial therapy (HAIAT) with evofosfamide in a rabbit model.

Experimental Design—VX2-tumor-bearing rabbits were assigned to 4 intraarterial therapy (IAT) groups (n=7/group): 1) saline (control); 2) evofosfamide (Evo); 3) doxorubicin-Lipiodol

Corresponding Author: Jean-François Geschwind, M.D., Chairman of the Department of Diagnostic Radiology and Biomedical Imaging, Yale University School of Medicine, Chairman's Office, 330 Cedar Street, TE 2-230, New Haven, CT 06520. Phone: +1 (203) 785-6938, Fax: +1 (203) 785-3024. jeff.geschwind@yale.edu.
R.D.: rafaelduran.md@gmail.com; S.M.: sahar.mirpour@gmail.com; V.P.: vpeku@hotmail.com; S.G.K: gshanmu1@jhmi.edu; C.F.B: cbrayton@jhmi.edu; T.C.C: tcornis3@jhmi.edu; B.G.: boris.gorodetski@charite.de; J.R.: jreyes9@jhmi.edu; J.C: j.chapiro@googlemail.com; R.E.S.: ruediger@schernthaner.eu; C.F.: cfranga1@jhu.edu; M.L.: ming.lin@philips.com; J.D.S: difeisun@gmail.com; C.P.H: chart@thresholdpharm.com.

Disclosures: B.G. and J.C.: Grant Support: Rolf W. Günther Foundation for Radiological Science. M.L.: Philips employee. J.D.S and C.P.H: former or current employees and stockholders of Threshold Pharmaceuticals, Inc. J.F.G: Consultant: Biocompatibles/BTG, Bayer HealthCare, Guerbet, Nordion/BTG, Philips Healthcare and Jennerex. Grant Support: Biocompatibles/BTG, Bayer HealthCare, Philips Medical, Nordion/BTG, Threshold, Guerbet, DOD, NCI-ECOG and NIH-R01. Founder and CEO PreScience Labs, LLC. The remaining authors have no conflict of interest and nothing to disclose.

Author Manuscript Author Manuscript Author Manuscript Author Manuscript

emulsion followed by embolization with 100-300μm beads (conventional, cTACE); or 4) cTACE and evofosfamide (cTACE+Evo). Blood samples were collected pre-IAT and 1/2/7/14 days post-IAT. A semiquantitative scoring system assessed hepatocellular damage. Tumor volumes were segmented on multidetector CT (baseline, 7/14 days post-IAT). Pathologic tumor necrosis was quantified using manual segmentation on whole slide images. Hypoxic fraction (HF) and compartment (HC) were determined by pimonidazole staining. Tumor DNA damage, apoptosis, cell proliferation, endogenous hypoxia and metabolism were quantified (γ-H2AX, annexin V, caspase-3, Ki-67, HIF1α, VEGF, GAPDH, MCT4 and LDH).

Results—cTACE+Evo showed a similar profile of liver enzymes elevation and pathologic scores compared to cTACE. Neither hematologic nor renal toxicity were observed. Animals treated with cTACE+Evo demonstrated smaller tumor volumes, lower tumor growth rates and higher necrotic fractions compared to cTACE. cTACE+Evo resulted in a marked reduction in the HF and HC. Correlation was observed between decreases in HF or HC and tumor necrosis. cTACE+Evo promoted antitumor effects as evidenced by increased expression of γ-H2A.X, apoptotic biomarkers and decreased cell proliferation. Increased HIF1α/VEGF expression and tumor glycolysis supported HAIAT.

Conclusion—HAIAT achieved a promising step towards the locoregional targeting of tumor hypoxia. The favorable toxicity profile and enhanced anticancer effects of evofosfamide in combination with cTACE pave the way towards clinical trials in patients with liver cancer.

Keywords

hypoxia-activated prodrug; TH-302; Evofosfamide; Hypoxia; TACE; VX2; Hepatocellular carcinoma

Introduction

Hypoxia is one of the most common and frequent physiological alteration of solid tumors, including hepatocellular carcinoma and has been strongly correlated with disease progression and resistance to chemotherapy (1, 2). In addition, tumor hypoxia has been shown to promote the emergence of a more aggressive and metastatic cancer phenotype (1, 3) which demonstrates increased resistance to apoptosis (4), stimulates angiogenesis (1) and favors cancer growth by altering cell metabolism (5). Overall, tumor hypoxia contributes to a poor clinical prognosis (6). As a result, a variety of hypoxia-targeted therapies have been developed including hypoxia-inducible factor 1 (HIF-1α) targeting, hypoxia-selective gene therapy, genetic engineering of anaerobic bacteria and hypoxia-activated prodrugs (HAPs) (2).

Among these different hypoxia-targeted strategies, HAPs are unique in that they are selectively activated under low oxygenation conditions, and remain as nontoxic prodrug during normoxic or aerobic conditions. This distinctive characteristic renders HAPs as potentially very effective in the setting of transarterial chemoembolization (TACE). Indeed, the embolic effect of TACE increases the hypoxic microenvironment of solid tumors and provides an attractive setting for selective activation of bioreductive prodrugs under low tissue oxygen state. Moreover, TACE allows for the loco-regional delivery of high-doses of

Author Manuscript Author Manuscript Author Manuscript Author Manuscript

chemotherapy that have the potential to reach distal tumor regions where hypoxic cells reside in a pharmacological sanctuary (7, 8). Furthermore, the use of HAPs in TACE could help mitigate detrimental effects triggered by the embolization with the activation of HIF-1α-dependent pathways, such as subsequent gene overexpression of vascular endothelial growth factor (VEGF) (9, 10) and hypoxia-induced chemoresistance (11).

Evofosfamide (formerly called TH-302), is a 2-nitroimidazole triggered HAP of the cytotoxin bromo-isophosphoramide mustard (12). Evofosfamide has shown broad-spectrum anticancer efficacy in multiple human cell lines and xenograft models (13-18) and is currently undergoing clinical evaluation (19-21).

The purpose of this study was to evaluate the safety and efficacy of hypoxia-activated intraarterial therapy (HAIAT) with evofosfamide in an orthotopic rabbit model of liver cancer.

MATERIALS AND METHODS

Animal Tumor Model

Adult female New Zealand white rabbits (Millbrook Breeding Labs, Amherst, MA) weighing 3.9-5.7 kg were used in accordance with institutional guidelines under approved animal care and use committee protocols from the Johns Hopkins University. The rabbit was chosen as it is considered the animal model of choice for intraarterial therapies to the liver (22). Food and water was allowed *ad libitum*. VX2 tumor chunks from previous experiments were injected into the hind legs of carrier rabbit and tumor was grown for 2 weeks. Each carrier was used to supply recipients for tumor implantation into the left liver lobe of the experimental rabbits as detailed in previous publication (23). The tumors were allowed to grow in the livers for 13–14 days (24).

Experimental Design

Animals were randomized into 4 hepatic intra-arterial treatment regimens and received an infusion of either: (a) normal saline (5 mL of 0.9% NaCl) (control group; n=7); (b) evofosfamide (Evo group; n=7); (c) an emulsion of doxorubicin (Sigma-Aldrich) and Lipiodol (Lipiodol Ultra-Fluide, Laboratoire Guerbet, Aulnay-sous-Bois, France) followed by embolization with 100-300 μm bland beads (Embospheres, Merit Medical Systems, South Jordan, UT) (conventional TACE - [cTACE] - group; n=7); (d) a combination of doxorubicin/Lipiodol emulsion and evofosfamide followed by embolization with 100-300 μm bland beads (cTACE+Evo group; n=7). Animals underwent multidetector computed tomography (MDCT) 24 hours pre-treatment and then at 7 and 14 days after the interventional treatment. Comprehensive blood work (complete liver, hematologic and renal panels) was obtained at baseline, 1, 2, 7 and 14 days after treatment. Daily clinical monitoring was performed. Three animals in each group were randomly sacrificed 2 days after treatment for histopathological and immunohistochemical analysis. The rest of the animals were sacrificed on day 14 after the last imaging assessment.

Author Manuscript Author Manuscript Author Manuscript Author Manuscript

Treatment Regimen

Evofosfamide was formulated in saline at 5 mg/mL and filtered through a 0.2 μm filter before animal dosing. Evofosfamide was prepared by study members who did not participate in the embolization procedures. A treatment dose of 7.7 mg/kg was used based on the FDA guidelines for dose translation based on body surface area and previous studies (14, 19-21, 25). Doxorubicin powder was reconstituted with saline immediately before intra-arterial injection, for a final concentration of 10 mg/mL. This dose calculation was based on the most common clinically administered doses of doxorubicin in the setting of cTACE (50 mg, for a ~70 kg person) (26). The doxorubicin solution was mixed to obtain a homogenous clear red solution. In a separate syringe, an equal-to-doxorubicin-solution volume of Lipiodol was withdrawn. The two solutions were mixed according to the push-and-pull method using a metallic stopcock. 0.6-0.8 mL of the emulsion (total doxorubicin dose: 3-4 mg) was administered (cTACE and cTACE+Evo groups) followed by a volume of up to 0.1-0.2 mL of 100-300 μm beads mixed with an equal volume of non-ionic contrast medium (Visipaque 320, GE Healthcare). In the cTACE+Evo group, the emulsion was injected following a sequential protocol. First a small volume of the emulsion (0.1-0.2 mL) was injected and pushed with saline to occlude distal tumor vessels and significantly slow down the arterial circulation. This was followed by a slow infusion of evofosfamide over a 10 min period after what the rest of the emulsion was administered completed by bland embolization. A sequential protocol was chosen to increase tumor hypoxic microenvironment due to distal occlusion of the tumor feeding arteries to enhance evofosfamide activation and lead to more efficient targeting of tumor hypoxia. Moreover, this sandwich injection technique that involves embolization before and after evofosfamide infusion may allow for a better activation of evofosfamide that is trapped is the embolized tissue to enhance antitumor efficacy. At the time of the embolization procedure, once the microcatheter was in the treatment position, the interventional radiologists were given the embolization material. At that time, the interventional radiologists could guess the actual treatment that was administered based on visual assessment (e.g. saline vs. Lipiodol + doxorubicin) and based on injection protocols. The interventional radiologists could not guess the actual treatment based on visual assessment or injection protocols when saline or evofosfamide alone were administered (both saline and evofosfamide alone are translucent).

Transarterial Chemoembolization Procedure

The interventional procedure was performed as previously reported (23, 24). Briefly, animals were pre-anesthetized with inhalant isoflurane (5%) on oxygen using a cone mask and anesthesia was then maintained via inhalant isoflurane (1.5-3%) on oxygen. Surgical cut down was done to gain access into the common femoral artery followed by the placement of a 3-French vascular sheath (Cook, Inc., Bloomington, IN). A 2.1/1.7-French microcatheter (Echelon 10, ev3 Endovascular, Inc., Plymouth, MN) was manipulated into the celiac axis, after which a celiac arteriogram was done to delineate the blood supply to the liver. The left hepatic artery was then selectively catheterized; this was occasionally performed with the aid of a steerable guide wire (0.014 in. Transcend wire; Boston Scientific Oncology, Natick, MA). The tumor was visualized on digital subtraction angiography as a region of hypervascular blush located in the left lobe of the liver. With the microcatheter in this position, the different treatment regimens were carefully administered under real-time

Author Manuscript Author Manuscript Author Manuscript Author Manuscript

fluoroscopy to prevent nontarget delivery. The endpoint of embolization was absence of forward flow (for cTACE and cTACE+Evo groups). Upon completion of the treatment, the microcatheter was removed, the common femoral artery was ligated and the surgical cut down was closed in one layer using absorbable suture material. Analgesic buprenorphine (0.02-0.05 mg/kg) was administered intramuscularly.

Safety Profile

Blood samples were collected from a marginal ear vein at baseline, 1, 2, 7 and 14 days after treatment to determine liver function. Potential hematologic (white blood cell, neutrophil, lymphocyte, monocyte, eosinophil and basophil counts and complete erythrocyte panel) or renal (creatinine, blood urea nitrogen, Na^+, K^+, Cl^-) toxicities were evaluated as well using standard enzymatic reaction.

Quantitative Image Analysis

Pre-anesthetized rabbits were scanned at baseline (24 hours before treatment), and at 7 and 14 days following treatment. Images were obtained with a 320-detector-row cardiac MDCT scanner (Aquillon One, Toshiba, Japan). As the coverage in the Z-direction was of 16 cm (320-detector-rows) the upper abdomen of the animals that includes the whole liver could be acquired with one gantry rotation with the table of the scanner remaining static. The large field of view and the fast image acquisition (scan time of 350 msec/360°) eliminates reconstruction artifacts allowing for high image quality (27). Unenhanced and contrast-enhanced scans were performed by intravenous injection of 1.5 mL/kg isoosmolar contrast medium (Isovue-370) at 1 mL/sec followed by a saline flush. Other imaging parameters were: 120 kVp, 350 mA, 0.5 mm slice thickness, 0.5 mm collimator, FOV 22×22 cm.

A semiautomatic 3D quantitative software (Medisys, Philips Research, Suresnes, France) was used to segment the tumors on the arterial phase of the MDCT scans and obtain the entire tumor volumes. The arterial phase was chosen due to the known hypervascular pattern of the tumors. This software uses non-Euclidean geometry and theory of radial basis functions which allows for highly precise segmentation of 3D objects with multiple shapes as described previously (28) (**Supplementary Figure S1**).

Histology and Immunohistochemistry

At 2 days or at the study end point (14 days after treatment), animals were sacrificed under deep anesthesia by i.v. injection of thiopental (100 mg/kg). To investigate the significance of the hypoxic fraction, pimonidazole (Hypoxyprobe, Inc., Burlington, MA) was intraperitoneally injected at 50 mg/kg two hours before sacrifice in three rabbits per group at 2 and 14 days after the interventional treatment (29). Rabbit livers were immediately harvested. The liver with the tumor was cut into 3 mm thick slices. Peritumoral treated and contralateral untreated liver parenchyma was also collected. Tissues were immediately placed in 10% buffered formalin. Subsequent complete necropsy (except brain) was done on all animals. Formalin-fixed tissue was paraffin-embedded and sectioned at 4 μm. Tissues slices were stained with hematoxylin and eosin (H&E) or processed for immunohistochemistry (IHC). IHC was performed on the specimens collected 2 days after

Author Manuscript Author Manuscript Author Manuscript Author Manuscript

treatment as early time points have shown to give optimal biomarkers expression to evaluate response to therapy (30, 31).

Tumor sections were evaluated for the following targets: HIF-1α (Thermo Scientific, Inc.), VEGF (Dako, Agilent Technologies, Inc.), γ-H2A.X (Santa Cruz Biotechnology, Inc.), annexin V (Santa Cruz), caspase-3 (Santa Cruz), Ki-67 (Dako), glyceraldehyde-3-phospahte dehydrogenase (GAPDH; Santa Cruz), monocarboxylate transporter 4 (MCT4; Santa Cruz), lactate dehydrogenase (LDH; Santa Cruz), and terminal deoxynucleotidyl transferase dUTP nick end labeling (TUNEL) using the TUNEL Apoptosis Detection Kit (Millipore). Specimens were deparaffinized using xylene and rehydrated using a descending ethanol dilution series. After washing with deionized water, samples were permeabilized in boiling retrieval solution containing citrate (Dako) for 40 min at 95°C. Specimens were cooled down to room temperature (RT) and incubated with 100 μl of Peroxidase Quenching Solution (Invitrogen) for 5 min, and incubated with 100 μl of Blocking Solution (Invitrogen) for 20 min. Incubation with primary antibodies (HIF-1α, 1:50; VEGF, 1:100; γ-H2A.X, 1:50; annexin V, 1:50; caspase-3, 1:50; Ki-67, 1:200; GAPDH, 1:500; MCT4, 1:50 ; LDH, 1:50; in PBS) occurred at RT in a moist chamber for 45-60 min. Mouse anti-goat (Santa Cruz; or goat anti-mouse (Bio-Rad) where so appropriate) IgG-HRP conjugated secondary antibody was added to the samples for 30 minutes in a moist chamber. 26.5 μl of 3,3'-diaminobenzidine (DAB) chromogen were mixed well in the dark with 1 mL of DAB Substrate Buffer and 100 μl were added to each specimen for 5 min. Hematoxylin was used as a counterstain. Incubation steps were followed by washing with distilled water and twice with PBS for 2 min each. Samples were sealed using antifade mountant (ProLong Gold Antifade, Life Technologies) and covered with a coverslip.

Quantitative Histological and Immunohistochemical Analysis

All histological slides (H&E, pimonidazole and other molecular targets) were digitized at 20x magnification using an Aperio ScanScope AT slide scanner (Leica Biosystems Inc., Vista, CA). Manual segmentation and image analysis was performed using the Aperio ImageScope® viewer.

H&E stained slides were used for tumor morphology and quantification of tumor necrosis. Pathologic tumor necrosis was quantified in the whole tumor. An experienced liver pathologist (C.F.B) who was blinded to all clinical and radiological data manually outlined in contiguous slides the whole tumor area and area of necrosis for each whole slide image (**Figure 1A**) (32). The necrotic fraction of each tumor was calculated as the percentage of the tumor necrotic area in the entire tumor.

To obtain objective and quantitative immunohistochemical analysis of tumor tissues, a color deconvolution image analysis algorithm was used as described in previous works (33-36). Briefly, the Color Deconvolution v9 and ImageScope software (Aperio®) were used to individually calibrate each staining in the disease-relevant areas (tumor tissues) that had been manually annotated. This process involved iterative adjustments of the deconvolution algorithm with various intensity thresholds for positivity. The resultant colormap was then compared to stained tissues and validated by an experienced pathologist (T.C.C) who was blinded to all clinical and radiological data to obtain concordance (**Figure 1B**). The metrics

Author Manuscript Author Manuscript Author Manuscript Author Manuscript

used for staining quantification were the percentage of positive pixels and the total tumor area, which was defined as the cumulative total area of combined positive and negative pixels. The hypoxic fraction (HF) was calculated in the viable tumor tissue with exclusion of tumor necrotic areas (HF = pimonidazole-positive area/viable tumor area). The hypoxic compartment (HC) was defined as the percentage of pimonidazole-positive area in the whole tumor area (16). HIF-1α, VEGF, γ-H2A.X, annexin V, caspase-3, GAPDH, MCT4, LDH positivity was evaluated in the whole tumor area. The Aperio nuclear V9 algorithm was used to quantitatively identify Ki-67-positive cells as previously described (33, 37).

Confocal fluorescence microscopy (LSM 700, Zeiss; EC Plan-Neofluar 40x/1.3 NA Oil lens DIC M27) was performed at 40x magnification for the TUNEL-stained tissue sections. A total of 5-10 fields were captured per section. Semi-quantitative image analysis was performed using the Bio-Formats Importer plugin of ImageJ (National Institutes of Health, Bethesda, MD).

Hepatocellular Damage Analysis

Targeted and contralateral untreated liver specimens were evaluated on H&E staining by an experienced pathologist (C.F.B.). The severity of liver injury, if any, was evaluated using a score adapted from Suzuki et al (38) and Kleiner et al (39). The scoring system comprised of 8 histological features that were assessed semi-quantitatively: hepatocellular necrosis (0-4), vacuolization (0-4), ballooning (0-2), lobular inflammation (0-4), steatosis (0-3), fibrosis (0-4), biliary hyperplasia (0-4) and granulation (0-4).

Statistical analysis

Animals were randomly assigned to treatment groups using randomization online software (GraphPad Software, La Jolla, CA). Experiment data were expressed as mean ± standard error of the mean (SEM). Measurements were compared among all four experimental groups using the Kruskal-Wallis test. For this and the other tests, significance levels were calculated, when possible, with exact methods based on the permutation distribution of the treatment labels, as these do not rely on normal approximations, in order to increase validity of the findings. Specifically, the slopes of the trajectories of log tumor volume over time (exponential growth) were estimated by Generalized Estimating Equations (40), and were compared across experimental groups using the exact distribution of the estimated slopes. The correlation of HF and HC with response to therapy across treatment groups was evaluated with the Pearson correlation coefficient r, and its significance was assessed in the distribution of r obtained by permuting the order of one of the two variables being correlated. Measurements between treated and untreated lobes across animals within treatment groups were compared with the exact distribution of the t-test obtained by permuting the treated and untreated values within each animal. A two-tailed *P*-value of less than 0.05 was considered statistically significant. A power analysis determined the sample size n=7/group was sufficient to detect with high probability the substantial treatment effects we had aimed to see in the study. For example, when comparing the volume trajectories for the 4 rabbits with trajectory data in cTACE to the 4 rabbits with trajectory in cTACE+Evo, the average slopes between the two groups differed by 4.4 standard deviations (effect size 4.4), and the power for detecting such difference with the exact test was greater than 97%.

Author Manuscript Author Manuscript Author Manuscript Author Manuscript

The power was still > 80% for effect sizes > 3. Statistical analysis was performed with two software packages (R: A Language and Environment for Statistical Computing, R Core Team, R Foundation for Statistical Computing, Vienna, Austria, 2013 and GraphPad Prism version 6.00, GraphPad Software, La Jolla, CA).

RESULTS

Safety

The safety profile of evofosfamide was determined by clinical evaluation, body weight measurements, serial blood work, and complete necropsy. Two animals from the control group were moribund at the study end point due to high tumor burden. Animals tolerated evofosfamide well with no apparent drug-induced toxicity determined by daily clinical assessment. There was no significant difference in body weight change among the groups. All treatment groups significantly increased plasma alanine aminotransferase and aspartate aminotransferase compared with vehicle control. The cTACE+Evo group had a similar profile in liver enzyme elevation compared to cTACE, although it was higher and more sustained. However this elevation was only statistically significant compared to cTACE at day 7 for alanine aminotransferase. All the tested liver enzymes returned to normal by day 14. Total bilirubin levels were slightly higher with cTACE+Evo but not statistically significant. The synthetic function of the liver remained unchanged throughout the experiment as shown by albumin levels (**Supplementary Figure S2**). Similar elevations of white blood cells were observed in all groups following the interventional procedure. Neither hematologic toxicity nor abnormal renal function was observed when evofosfamide (7.7 mg/kg) was intraarterially delivered either alone or in combination with cTACE (data not shown). As a target organ, the liver exhibited morphologic change by H&E staining and hypoxia change by pimonidazole staining. In normal nontumoral liver, there was a gradient of hypoxia radiating outwards from portal triads, but after the embolization treatment (cTACE and cTACE+Evo groups), hypoxic extent and intensity was dramatically increased (**Supplementary Figure S3a**). Besides the targeted liver, there was no other organ abnormalities noted during necropsy (**Supplementary Figure S3b**).

Hepatocellular Damage

The extent of hepatocellular damage was investigated with a dedicated liver tissue scoring system. Evo and cTACE demonstrated similar toxicity when analyzing the liver parenchyma around the tumors, supporting the fact that evofosfamide is activated in less oxygenated tumor areas and its released effector diffuses locoregionally beyond hypoxic areas, consistent with a bystander effect. Most importantly, similar scores were obtained between cTACE and those of cTACE+Evo. However upon analyzing the subgroup of animals at day 14, lobular inflammation was more pronounced in the combination therapy (average 2.5 points higher; $P = 0.028$) (**Table 1**).

Anticancer Effect of Evofosfamide by Quantitative Imaging

The anticancer efficacy of evofosfamide was evaluated using quantitative volumetric image analysis. Compared with the control group, Evo treated tumors were significantly smaller at 7 and 14 days (4.6±0.7 vs. 1.5±0.5 cm^3 and 15.9±3.2 vs. 2.8±0.9 cm^3, respectively). At day

Author Manuscript Author Manuscript Author Manuscript Author Manuscript

14, both chemoembolization groups showed smaller volumes compared to the Evo group. Importantly, cTACE+Evo demonstrated significantly smaller volumes than cTACE alone (0.31±0.08 vs. 0.8±0.07 cm^3, respectively) (**Figure 2A**). At day 14, Evo achieved significantly reduced tumor growth rate compared to control and similar tumor growth rate to cTACE (**Figure 2B**). cTACE+Evo outperformed the other treatment groups by achieving not only significantly lower tumor growth rate but also tumor shrinkage (**Figure 2B**). By permutation-based linear regression assuming dependent observations, tumor growth slopes between cTACE (+0.04) and cTACE+Evo (−0.11) were significantly different ($P = 0.027$). cTACE+Evo achieved a reduction in tumor volume of 50% by day 9, whereas the calculated tumor volume doubling time in the cTACE group was 25 days (**Figure 2C**).

Anticancer Effect of Evofosfamide by Quantitative Pathology

Pathologic tumor necrosis was quantified by slide-by-slide histosegmentation to investigate the entire tumors. When compared to vehicle, histopathologic analysis performed at day 2 showed increased tumor necrosis in the treatment groups (87.5±12.1%, 97.5±1.1% and 97.5±0.8% with Evo, cTACE, cTACE+Evo, respectively) (**Figure 3A**). At day 14, the combination therapy with cTACE+Evo demonstrated significantly more necrotic fraction compared to vehicle, Evo alone and cTACE (**Figure 3B**).

Anticancer Effect of Evofosfamide by Hypoxia Targeting

Tumor hypoxic regions were detected by pimonidazole staining and quantified by color deconvolution algorithm. The HF and the HC changed significantly post intraarterial therapy ($R^2 = 76\%$, $P = 0.002$ and $R^2 = 95\%$, $P = 0.005$, respectively) (**Figure 4**). To further characterize this significance, we examined which subgrouping showed the next highest R-square. Tumors treated with cTACE+Evo had a significantly lower HF compared to Evo alone and cTACE groups ($P = 0.037$) (**Figure 4B**). Regarding the magnitude of hypoxia in the whole tumor, Evo alone and cTACE+Evo demonstrated a significantly lower HC compared to the vehicle ($P = 0.037$) and a clear trend compared to cTACE ($P = 0.07$), indicating antitumor efficacy of hypoxia targeting by evofosfamide (**Figure 4C**). To further investigate the relationship between tumor hypoxia and treatment response, a correlation analysis was performed using exact permutations distribution to increase the validity of the findings. A significant negative correlation was found across treatment groups between the HF and the magnitude of the necrotic fraction at day 2 (Pearson's $r = -0.753$; $P = 0.004$). As well, the decrease in the HC showed a strong negative correlation with tumor necrosis (Pearson's $r = -0.826$; $P = 0.001$).

At day 14 post intraarterial therapy, no difference in the HF was noted ($P = 0.11$) (**Figure 4E**). However, the HC was significantly different between the groups ($R^2 = 81\%$, $P = 0.026$). The HC of cTACE+Evo remained significantly lower compared to the other groups. Interestingly, the Evo group showed a significantly higher HC compared to the other groups (**Figure 4F**).

Author Manuscript Author Manuscript Author Manuscript Author Manuscript

Evofosfamide Induces DNA Damage, Promotes Apoptosis and Decreases Cellular Proliferation

The phosphorylation of the histone H2A.X (γ-H2A.X) variant was investigated to evaluate whether evofosfamide produces DNA crosslinking damage. γ-H2A.X was significantly upregulated in the tumors recovered at 2 days after therapy (R^2 = 85%, $P < 0.001$). The chemoembolization groups (cTACE and cTACE+Evo) demonstrated a significant increase expression of γ-H2A.X compared to control and Evo groups. This expression was significantly higher for cTACE+Evo compared to the Evo and cTACE groups (**Figure 5B**). Similarly, a marked increase of the apoptotic biomarkers annexin V and caspase-3 was achieved by evofosfamide and to a higher extent by the chemoembolization groups. The combination therapy demonstrated a significant increase in caspase-3 expression compared to the Evo and cTACE groups (**Figure 5C-D**). Importantly, all tumors in the cTACE+Evo group showed higher expression of γ-H2A.X, annexin V and caspase-3 compared to the tumors treated with cTACE. Following treatment with Evo and cTACE+Evo, expression of TUNEL was increased significantly above control levels (**Figure 5E**). Compared to cTACE, cTACE+Evo showed more advanced apoptotic stage with nuclear fragmentation resulting in semi-quantitative decreased pixel intensity (**Figure 5E**). Cell proliferation decreased in all treatment groups compared to controls. This reduction in cell proliferation was significantly more pronounced in tumors treated with Evo and cTACE+Evo compared to control and more importantly compared to cTACE alone (**Figure 5F**).

Tumor Metabolism

The upregulation of HIF-1α was significantly increased in the chemoembolization groups compared to controls indicating increase in the hypoxic microenvironment resulting from TACE. To investigate tumor glycolysis in the setting of HAIAT with procedure induced ischemia/hypoxia, key indicators of glycolysis such as LDH, GADPH and, the lactate transporter, MCT4 (41) were evaluated. Marked increase in the expression of MCT4 and LDH were observed in the cTACE and cTACE+Evo groups (**Figure 6**).

DISCUSSION

The main finding of this study is that hepatic HAIAT with evofosfamide as a single agent and more importantly in combination with cTACE achieved strong anticancer effects in the rabbit tumor liver model with minimal toxicity. Our data demonstrate a significant correlation between hypoxia-targeting and antitumor activity further supporting the anticancer potential of the locoregional delivery of the HAP technology.

Tumor hypoxia constitutes one of the main Achilles' heel of anticancer therapy. Thus, the development of therapeutic strategies such as HAPs to target tumor hypoxia is of utmost clinical relevance and importance. Evofosfamide has demonstrated anticancer efficacy *in vitro* and in xenograft models (13-18) and is currently undergoing clinical evaluation as a systemic chemotherapy agent (19-21). Here we investigated the locoregional delivery of evofosfamide in the setting of TACE by characterizing its safety and toxicity profile and quantifying its antitumor activity using different mechanistic approaches.

Author Manuscript Author Manuscript Author Manuscript Author Manuscript

In clinical practice, determination of liver function after locoregional therapy is critical for treatment toxicity evaluation and patient selection to identify candidates who would benefit from repeated therapy. Evo alone showed a slight increase in liver enzymes with rapid return to baseline within 2 days of therapy. As expected, a transient increase of liver enzymes was observed in the chemoembolization groups reaching a peak 1-2 days after treatment. cTACE +Evo showed a similar, although more pronounced, rise in liver enzymes when compared to cTACE. However, only alanine aminotransferase levels were significantly higher at day 7. Moreover, the histological toxicity scores were similar between cTACE+Evo and cTACE alone, with the exception of lobular inflammation being more pronounced at day 14 in the combination therapy group. In the clinic a majority of TACE procedures are performed in patients with liver cirrhosis. Although the rabbit constitutes the animal model of choice to investigate intraarterial therapies to the liver, baseline liver function is normal and no cirrhosis is present (22). Thus, the impact on liver function of the addition of Evo to cTACE in the setting of liver cirrhosis is yet to be assessed. Of note, no hematologic toxicity was observed, whereas such toxicity constitutes a known limitation of systemic therapy with evofosfamide (19-21). Taken together, these results demonstrate that evofosfamide alone and in combination with cTACE has a favorable toxicity profile with no compromise of liver metabolic and synthetic functions.

Using quantitative imaging and histopathological analysis of the whole tumor, we demonstrated that cTACE+Evo had a stronger anticancer efficacy than cTACE alone. cTACE was able to achieve a good local control of the tumors with low tumor volumes and tumor growth rate. However the addition of evofosfamide to cTACE enhanced antitumor efficacy. Specifically, cTACE+Evo outperformed the other treatment groups by not only resulting in significantly smaller tumor volumes and lower tumor growth rates but also actual tumor shrinkage. Of note, cTACE+Evo achieved consistent results in all treated animals at all observed time points when compared to cTACE and Evo alone, as illustrated by the consistently high necrotic fraction. This added efficacy of the combination therapy over cTACE alone could be beneficial in patients to achieve better local tumor control rate and improve current outcomes. In addition, the correlation analysis demonstrated a significant negative correlation between the necrotic fraction and the magnitude of the HF and the HC, further validating the antitumor activity of evofosfamide and underlining the relationship between tumor hypoxia targeting and treatment response. Interestingly, the hypoxic environment of control tumors decreased over time. It is possible that the development of tumor vessels was unable to meet the perfusion demand imposed by a rapidly growing and expanding tumor such as the VX2. As a result, oxygen and nutrients deprivation induced extensive tumor necrotic areas. An unexpected result was observed in the Evo group with increased HC at day 14. This may be explained by Evo potentially interfering with HIF-1α-dependent pathways such as VEGF-related angiogenesis with subsequent decreased vessels recruitment (42). In addition, once activated evofosfamide may have locoregionally diffused and damaged distal tumor vessels contributing to a subsequent increase in the hypoxic tumor microenvironment (43). While these findings deserve further investigations, they also evidence an opportunity for repeated therapy.

To further characterize the antitumor efficacy of evofosfamide, we quantitatively evaluated the expression of γ-H2A.X, annexin V, caspase-3, TUNEL and Ki-67. The ability of Evo to

Author Manuscript Author Manuscript Author Manuscript Author Manuscript

induce cross-linking DNA damage has also been reported in a murine model with the prodrug being delivered systemically (16). The expression of γ-H2A.X was mainly seen near hypoxic areas. Our data demonstrated that evofosfamide alone or in combination therapy with Lipiodol/doxorubicin-based chemoembolization not only achieved strong antitumor activity in tumor hypoxia but also in normoxic tumor regions located close to blood vessels. These findings suggest strong activation of the prodrug and diffusion to nearby tumor tissues consistent with a bystander effect (15, 44). When evofosfamide was given alone, this phenomenon was probably the main trigger for cell death while selective catheterization with decreased forward blood flow during drug delivery could have enhanced the activation of the bioreductive prodrug. Moreover, the generation of superoxides by evofosfamide could have contributed to part of the observed γ-H2A.X expression. Indeed, Meng et al (15) demonstrated that superoxide is generated under normoxic conditions by the redox cycling of evofosfamide through its one-electron reduction to the radical anion with subsequent reoxidization by oxygen back to the original prodrug configuration (15). The authors showed that a 100X-higher concentration of evofosfamide was necessary under normoxia compared to hypoxic conditions to achieve similar H2A.X expression (15). As intraarterially delivered evofosfamide reaches much higher concentration than evofosfamide given systemically, this could have contributed in part to the γ-H2A.X expression in our study. Furthermore, similar to γ-H2A.X, evofosfamide also induced the expression of apoptotic markers with a concomitant decrease in cell proliferation substantiating the efficacy of locoregional delivery.

Iatrogenic increase of hypoxic tumor microenvironment (i.e. by the embolization), as demonstrated here by HIF-1α upregulation and also previously reported (10, 45-49), together with increased reliance on anaerobic glycolysis by tumor cells (50), as shown by increased expression of MCT4 and LDH, provide a mechanistic explanation of the added anticancer efficacy of cTACE+Evo over cTACE and further validate TACE as an ideal setting for selective targeting of tumor hypoxia. Increased expression of HIF-1α and VEGF observed in the Evo group could potentially be explained by decreased forward blood flow around the microcatheter during superselective catheterization with consecutive increase in tumor hypoxia.

Anticancer drugs must access and diffuse into the extravascular space to reach the tumor microenvironment and cancer cells. To achieve efficacy, therapeutic drug concentrations must be reached. Doxorubicin is the most widely used cytotoxic drug in TACE. When given systemically, doxorubicin has a poor penetration through cancer tissue due to its avid binding to DNA and sequestration in endosomes by perivascular cells (51, 52). However, intraarterial administration of doxorubicin with TACE demonstrated improved drug penetration into tumor tissue compared to systemic therapy (53). Evofosfamide showed the ability to enhance the activity of commonly used systemic chemotherapeutics agents, notably doxorubicin, in xenograft models (14, 44). In patients with soft tissue sarcoma, doxorubicin combined with evofosfamide achieved a better outcome than doxorubicin alone (19). Here we demonstrated that evofosfamide combined with cTACE achieved better anticancer efficacy than cTACE supporting the added benefit of combining doxorubicin and evofosfamide as reported in preclinical and clinical studies (14, 19, 44).

Author Manuscript Author Manuscript Author Manuscript Author Manuscript

Because cancer cells are located at greater distances from the microvasculature than normal cells, the efficacy of hypoxic cytotoxins may be decreased by their limited diffusion into the extravascular tumor tissue to reach the hypoxic cancer cells (8, 54). Several hypoxia-activated prodrugs have progressed to clinical trials; however, none has yet been granted approval for clinical use, reflecting some challenges in the use of these novel drugs. Indeed hypoxia-independent cytotoxicity, low diffusion and short plasma half-life are some of the limitations of the bioreductive drug technology (54-56). Evofosfamide has shown an optimized profile with good drug penetrability and hypoxia-selective cytotoxicity with no evidence of hypoxia-independent targeting (15).

Taken together, our preclinical data support the hypothesis that tumor hypoxia can be an exploitable target for liver tumors by HAIAT. Hepatic HAIAT holds promise by several methodological strengths: 1) It allows for locoregional delivery of high concentration of the hypoxia-activated prodrug that could otherwise not be achieved by systemic delivery, potentially overcoming excessive metabolic consumption (diffusion-limited [chronic] hypoxia) (54). 2) Ischemia induced by the therapeutic embolization offers an ideal mechanistic setting for hypoxia-activated prodrug. 3) The tumor hypoxic microenvironment can be modified perprocedure by selective catheterization and sequential injection protocols like those used in this study or using devices such as balloon occlusion catheters in future research (e.g. temporary occlusion of the tumor feeding artery before drug delivery to intentionally increase tumor hypoxia) which potentially could enhance drug efficacy (perfusion-limited [acute] hypoxia) and lead to more efficient targeting of hypoxia.

In conclusion, preclinical benefit of HAIAT with evofosfamide was observed in liver cancer. HAIAT is a promising step towards locoregional targeting of tumor hypoxia. The favorable toxicity profile and strong anti-cancer effects of evofosfamide in combination with cTACE pave the way towards clinical trials in patient with liver cancer.

Supplementary Material

Refer to Web version on PubMed Central for supplementary material.

Acknowledgments

Financial Support: This study was funded by NIH/NCI R01 CA160771 and Threshold Pharmaceuticals, Inc.

Abbreviations and acronyms

HAPs	hypoxia-activated prodrugs
TACE	transarterial chemoembolization
HAIAT	hypoxia-activated intraarterial therapy
MDCT	multidetector computed tomography
IHC	immunohistochemistry
HF	hypoxic fraction

Author Manuscript Author Manuscript Author Manuscript Author Manuscript

HC hypoxic compartment

REFERENCES

1. Harris AL. Hypoxia--a key regulatory factor in tumour growth. Nature reviews Cancer. 2002; 2:38–47. [PubMed: 11902584]
2. Brown JM, Wilson WR. Exploiting tumour hypoxia in cancer treatment. Nature reviews Cancer. 2004; 4:437–47. [PubMed: 15170446]
3. Lunt SJ, Chaudary N, Hill RP. The tumor microenvironment and metastatic disease. Clin Exp Metastasis. 2009; 26:19–34. [PubMed: 18543068]
4. Graeber TG, Osmanian C, Jacks T, Housman DE, Koch CJ, Lowe SW, et al. Hypoxia-mediated selection of cells with diminished apoptotic potential in solid tumours. Nature. 1996; 379:88–91. [PubMed: 8538748]
5. Semenza GL. Regulation of cancer cell metabolism by hypoxia-inducible factor 1. Seminars in cancer biology. 2009; 19:12–6. [PubMed: 19114105]
6. Vaupel P, Mayer A. Hypoxia in cancer: significance and impact on clinical outcome. Cancer metastasis reviews. 2007; 26:225–39. [PubMed: 17440684]
7. Tredan O, Galmarini CM, Patel K, Tannock IF. Drug resistance and the solid tumor microenvironment. J Natl Cancer Inst. 2007; 99:1441–54. [PubMed: 17895480]
8. Minchinton AI, Tannock IF. Drug penetration in solid tumours. Nature reviews Cancer. 2006; 6:583–92. [PubMed: 16862189]
9. Shim JH, Park JW, Kim JH, An M, Kong SY, Nam BH, et al. Association between increment of serum VEGF level and prognosis after transcatheter arterial chemoembolization in hepatocellular carcinoma patients. Cancer science. 2008; 99:2037–44. [PubMed: 19016764]
10. Sergio A, Cristofori C, Cardin R, Pivetta G, Ragazzi R, Baldan A, et al. Transcatheter arterial chemoembolization (TACE) in hepatocellular carcinoma (HCC): the role of angiogenesis and invasiveness. The American journal of gastroenterology. 2008; 103:914–21. [PubMed: 18177453]
11. Poon RT, Lau C, Yu WC, Fan ST, Wong J. High serum levels of vascular endothelial growth factor predict poor response to transarterial chemoembolization in hepatocellular carcinoma: a prospective study. Oncology reports. 2004; 11:1077–84. [PubMed: 15069550]
12. Duan JX, Jiao H, Kaizerman J, Stanton T, Evans JW, Lan L, et al. Potent and highly selective hypoxia-activated achiral phosphoramidate mustards as anticancer drugs. Journal of medicinal chemistry. 2008; 51:2412–20. [PubMed: 18257544]
13. Hu J, Handisides DR, Van Valckenborgh E, De Raeve H, Menu E, Vande Broek I, et al. Targeting the multiple myeloma hypoxic niche with TH-302, a hypoxia-activated prodrug. Blood. 2010; 116:1524–7. [PubMed: 20530289]
14. Liu Q, Sun JD, Wang J, Ahluwalia D, Baker AF, Cranmer LD, et al. TH-302, a hypoxia-activated prodrug with broad in vivo preclinical combination therapy efficacy: optimization of dosing regimens and schedules. Cancer chemotherapy and pharmacology. 2012; 69:1487–98. [PubMed: 22382881]
15. Meng F, Evans JW, Bhupathi D, Banica M, Lan L, Lorente G, et al. Molecular and cellular pharmacology of the hypoxia-activated prodrug TH-302. Molecular cancer therapeutics. 2012; 11:740–51. [PubMed: 22147748]
16. Sun JD, Liu Q, Wang J, Ahluwalia D, Ferraro D, Wang Y, et al. Selective tumor hypoxia targeting by hypoxia-activated prodrug TH-302 inhibits tumor growth in preclinical models of cancer. Clin Cancer Res. 2012; 18:758–70. [PubMed: 22184053]
17. Hu J, Van Valckenborgh E, Xu D, Menu E, De Raeve H, De Bryune E, et al. Synergistic induction of apoptosis in multiple myeloma cells by bortezomib and hypoxia-activated prodrug TH-302, in vivo and in vitro. Molecular cancer therapeutics. 2013; 12:1763–73. [PubMed: 23832122]
18. Portwood S, Lal D, Hsu YC, Vargas R, Johnson MK, Wetzler M, et al. Activity of the hypoxia-activated prodrug, TH-302, in preclinical human acute myeloid leukemia models. Clin Cancer Res. 2013; 19:6506–19. [PubMed: 24088735]

Author Manuscript Author Manuscript Author Manuscript Author Manuscript

19. Ganjoo KN, Cranmer LD, Butrynski JE, Rushing D, Adkins D, Okuno SH, et al. A phase I study of the safety and pharmacokinetics of the hypoxia-activated prodrug TH-302 in combination with doxorubicin in patients with advanced soft tissue sarcoma. Oncology. 2011; 80:50–6. [PubMed: 21625179]
20. Weiss GJ, Infante JR, Chiorean EG, Borad MJ, Bendell JC, Molina JR, et al. Phase 1 study of the safety, tolerability, and pharmacokinetics of TH-302, a hypoxia-activated prodrug, in patients with advanced solid malignancies. Clin Cancer Res. 2011; 17:2997–3004. [PubMed: 21415214]
21. Chawla SP, Cranmer LD, Van Tine BA, Reed DR, Okuno SH, Butrynski JE, et al. Phase II Study of the Safety and Antitumor Activity of the Hypoxia-Activated Prodrug TH-302 in Combination With Doxorubicin in Patients With Advanced Soft Tissue Sarcoma. J Clin Oncol. 2014; 32:3299–306. [PubMed: 25185097]
22. Moreira PL, An YH. Animal models for therapeutic embolization. Cardiovasc Intervent Radiol. 2003; 26:100–10. [PubMed: 12677466]
23. Hong K, Khwaja A, Liapi E, Torbenson MS, Georgiades CS, Geschwind JF. New intra-arterial drug delivery system for the treatment of liver cancer: preclinical assessment in a rabbit model of liver cancer. Clin Cancer Res. 2006; 12:2563–7. [PubMed: 16638866]
24. Geschwind JF, Ko YH, Torbenson MS, Magee C, Pedersen PL. Novel therapy for liver cancer: direct intraarterial injection of a potent inhibitor of ATP production. Cancer Res. 2002; 62:3909–13. [PubMed: 12124317]
25. Reagan-Shaw S, Nihal M, Ahmad N. Dose translation from animal to human studies revisited. FASEB journal : official publication of the Federation of American Societies for Experimental Biology. 2008; 22:659–61. [PubMed: 17942826]
26. Marelli L, Stigliano R, Triantos C, Senzolo M, Cholongitas E, Davies N, et al. Transarterial therapy for hepatocellular carcinoma: which technique is more effective? A systematic review of cohort and randomized studies. Cardiovasc Intervent Radiol. 2007; 30:6–25. [PubMed: 17103105]
27. Xu L, Yang L, Fan Z, Yu W, Lv B, Zhang Z. Diagnostic performance of 320-detector CT coronary angiography in patients with atrial fibrillation: preliminary results. Eur Radiol. 2011; 21:936–43. [PubMed: 21153826]
28. Mory B, Ardon R, Yezzi AJ, Thiran JP. Non-Euclidean Image-Adaptive Radial Basis Functions for 3D Interactive Segmentation. Ieee I Conf Comp Vis. 2009:787–94.
29. Raleigh JA, Calkins-Adams DP, Rinker LH, Ballenger CA, Weissler MC, Fowler WC Jr. et al. Hypoxia and vascular endothelial growth factor expression in human squamous cell carcinomas using pimonidazole as a hypoxia marker. Cancer Res. 1998; 58:3765–8. [PubMed: 9731480]
30. Saggar JK, Fung AS, Patel KJ, Tannock IF. Use of molecular biomarkers to quantify the spatial distribution of effects of anticancer drugs in solid tumors. Molecular cancer therapeutics. 2013; 12:542–52. [PubMed: 23348047]
31. Wilson GK, Tennant DA, McKeating JA. Hypoxia inducible factors in liver disease and hepatocellular carcinoma: Current understanding and future directions. J Hepatol. 2014
32. Chapiro J, Wood LD, Lin M, Duran R, Cornish T, Lesage D, et al. Radiologic-pathologic analysis of contrast-enhanced and diffusion-weighted MR imaging in patients with HCC after TACE: diagnostic accuracy of 3D quantitative image analysis. Radiology. 2014; 273:746–58. [PubMed: 25028783]
33. Ruifrok AC, Johnston DA. Quantification of histochemical staining by color deconvolution. Analytical and quantitative cytology and histology / the International Academy of Cytology [and] American Society of Cytology. 2001; 23:291–9.
34. Krajewska M, Smith LH, Rong J, Huang X, Hyer ML, Zeps N, et al. Image analysis algorithms for immunohistochemical assessment of cell death events and fibrosis in tissue sections. The journal of histochemistry and cytochemistry : official journal of the Histochemistry Society. 2009; 57:649–63. [PubMed: 19289554]
35. Brennan DJ, Rexhepaj E, O'Brien SL, McSherry E, O'Connor DP, Fagan A, et al. Altered cytoplasmic-to-nuclear ratio of survivin is a prognostic indicator in breast cancer. Clin Cancer Res. 2008; 14:2681–9. [PubMed: 18451232]

Author Manuscript Author Manuscript Author Manuscript Author Manuscript

36. Krajewska M, Kitada S, Winter JN, Variakojis D, Lichtenstein A, Zhai D, et al. Bcl-B expression in human epithelial and nonepithelial malignancies. Clin Cancer Res. 2008; 14:3011–21. [PubMed: 18483366]
37. Samols MA, Smith NE, Gerber JM, Vuica-Ross M, Gocke CD, Burns KH, et al. Software-automated counting of Ki-67 proliferation index correlates with pathologic grade and disease progression of follicular lymphomas. American journal of clinical pathology. 2013; 140:579–87. [PubMed: 24045557]
38. Suzuki S, Toledo-Pereyra LH, Rodriguez FJ, Cejalvo D. Neutrophil infiltration as an important factor in liver ischemia and reperfusion injury. Modulating effects of FK506 and cyclosporine. Transplantation. 1993; 55:1265–72. [PubMed: 7685932]
39. Kleiner DE, Brunt EM, Van Natta M, Behling C, Contos MJ, Cummings OW, et al. Design and validation of a histological scoring system for nonalcoholic fatty liver disease. Hepatology. 2005; 41:1313–21. [PubMed: 15915461]
40. Liang KY, Zeger SL. Longitudinal Data-Analysis Using Generalized Linear-Models. Biometrika. 1986; 73:13–22.
41. Ullah MS, Davies AJ, Halestrap AP. The plasma membrane lactate transporter MCT4, but not MCT1, is up-regulated by hypoxia through a HIF-1alpha-dependent mechanism. The Journal of biological chemistry. 2006; 281:9030–7. [PubMed: 16452478]
42. von Marschall Z, Cramer T, Hocker M, Finkenzeller G, Wiedenmann B, Rosewicz S. Dual mechanism of vascular endothelial growth factor upregulation by hypoxia in human hepatocellular carcinoma. Gut. 2001; 48:87–96. [PubMed: 11115828]
43. Sun JD, Ahluwalia D, Liu Q, Li W, Wang Y, Meng F, et al. Combination treatment with hypoxia-activated prodrug evofosfamide (TH-302) and mTOR inhibitors results in enhanced antitumor efficacy in preclinical renal cell carcinoma models. American journal of cancer research. 2015; 5:2139–55. [PubMed: 26328245]
44. Saggar JK, Tannock IF. Activity of the hypoxia-activated pro-drug TH-302 in hypoxic and perivascular regions of solid tumors and its potential to enhance therapeutic effects of chemotherapy. Int J Cancer. 2014; 134:2726–34. [PubMed: 24338277]
45. Li X, Feng GS, Zheng CS, Zhuo CK, Liu X. Expression of plasma vascular endothelial growth factor in patients with hepatocellular carcinoma and effect of transcatheter arterial chemoembolization therapy on plasma vascular endothelial growth factor level. World journal of gastroenterology : WJG. 2004; 10:2878–82. [PubMed: 15334691]
46. Suzuki H, Mori M, Kawaguchi C, Adachi M, Miura S, Ishii H. Serum vascular endothelial growth factor in the course of transcatheter arterial embolization of hepatocellular carcinoma. International journal of oncology. 1999; 14:1087–90. [PubMed: 10339662]
47. Liang B, Zheng CS, Feng GS, Wu HP, Wang Y, Zhao H, et al. Correlation of hypoxia-inducible factor 1alpha with angiogenesis in liver tumors after transcatheter arterial embolization in an animal model. Cardiovasc Intervent Radiol. 2010; 33:806–12. [PubMed: 19937023]
48. Virmani S, Rhee TK, Ryu RK, Sato KT, Lewandowski RJ, Mulcahy MF, et al. Comparison of hypoxia-inducible factor-1alpha expression before and after transcatheter arterial embolization in rabbit VX2 liver tumors. J Vasc Interv Radiol. 2008; 19:1483–9. [PubMed: 18922400]
49. Liao XF, Yi JL, Li XR, Deng W, Yang ZF, Tian G. Angiogenesis in rabbit hepatic tumor after transcatheter arterial embolization. World journal of gastroenterology : WJG. 2004; 10:1885–9. [PubMed: 15222029]
50. Yasuda S, Arii S, Mori A, Isobe N, Yang W, Oe H, et al. Hexokinase II and VEGF expression in liver tumors: correlation with hypoxia-inducible factor 1 alpha and its significance. J Hepatol. 2004; 40:117–23. [PubMed: 14672622]
51. Lankelma J, Dekker H, Luque FR, Luykx S, Hoekman K, van der Valk P, et al. Doxorubicin gradients in human breast cancer. Clin Cancer Res. 1999; 5:1703–7. [PubMed: 10430072]
52. Primeau AJ, Rendon A, Hedley D, Lilge L, Tannock IF. The distribution of the anticancer drug Doxorubicin in relation to blood vessels in solid tumors. Clin Cancer Res. 2005; 11:8782–8. [PubMed: 16361566]

Author Manuscript Author Manuscript Author Manuscript Author Manuscript

53. Liang B, Xiong F, Wu H, Wang Y, Dong X, Cheng S, et al. Effect of transcatheter intraarterial therapies on the distribution of Doxorubicin in liver cancer in a rabbit model. PLoS One. 2013; 8:e76388. [PubMed: 24116106]

54. Hicks KO, Pruijn FB, Secomb TW, Hay MP, Hsu R, Brown JM, et al. Use of three-dimensional tissue cultures to model extravascular transport and predict in vivo activity of hypoxia-targeted anticancer drugs. J Natl Cancer Inst. 2006; 98:1118–28. [PubMed: 16912264]

55. Phillips RM, Hendriks HR, Peters GJ, Pharmacology E, Molecular Mechanism G. EO9 (Apaziquone): from the clinic to the laboratory and back again. British journal of pharmacology. 2013; 168:11–8. [PubMed: 22509926]

56. Guise CP, Abbattista MR, Singleton RS, Holford SD, Connolly J, Dachs GU, et al. The bioreductive prodrug PR-104A is activated under aerobic conditions by human aldo-keto reductase 1C3. Cancer Res. 2010; 70:1573–84. [PubMed: 20145130]

Author Manuscript Author Manuscript Author Manuscript Author Manuscript

Translational Relevance

Tumor hypoxia has long been considered as one of the main challenges of anticancer therapy. As a result, hypoxia-activated therapies have been developed and hold promise in achieving meaningful results once translated to the clinic. The use of hypoxia-activated prodrugs in the setting of transarterial chemoembolization (TACE) is particularly appealing as it allows loco-regional delivery of high-doses of chemotherapy that have the potential to reach distal tumor regions where hypoxic cells reside in a pharmacological sanctuary. Moreover the embolic effect of TACE provides an attractive setting for selective activation of bioreductive prodrugs. The main finding of this study is that TACE in combination with evofosfamide achieved enhanced anticancer efficacy with limited additive toxicity compared to TACE alone. The observed correlation between the magnitude of hypoxia and evofosfamide efficacy established the *in vivo* proof-of-concept of selective hypoxia-activated intraarterial therapy for liver cancer. The results of this study suggest that clinical trials should be considered.

Author Manuscript Author Manuscript Author Manuscript Author Manuscript

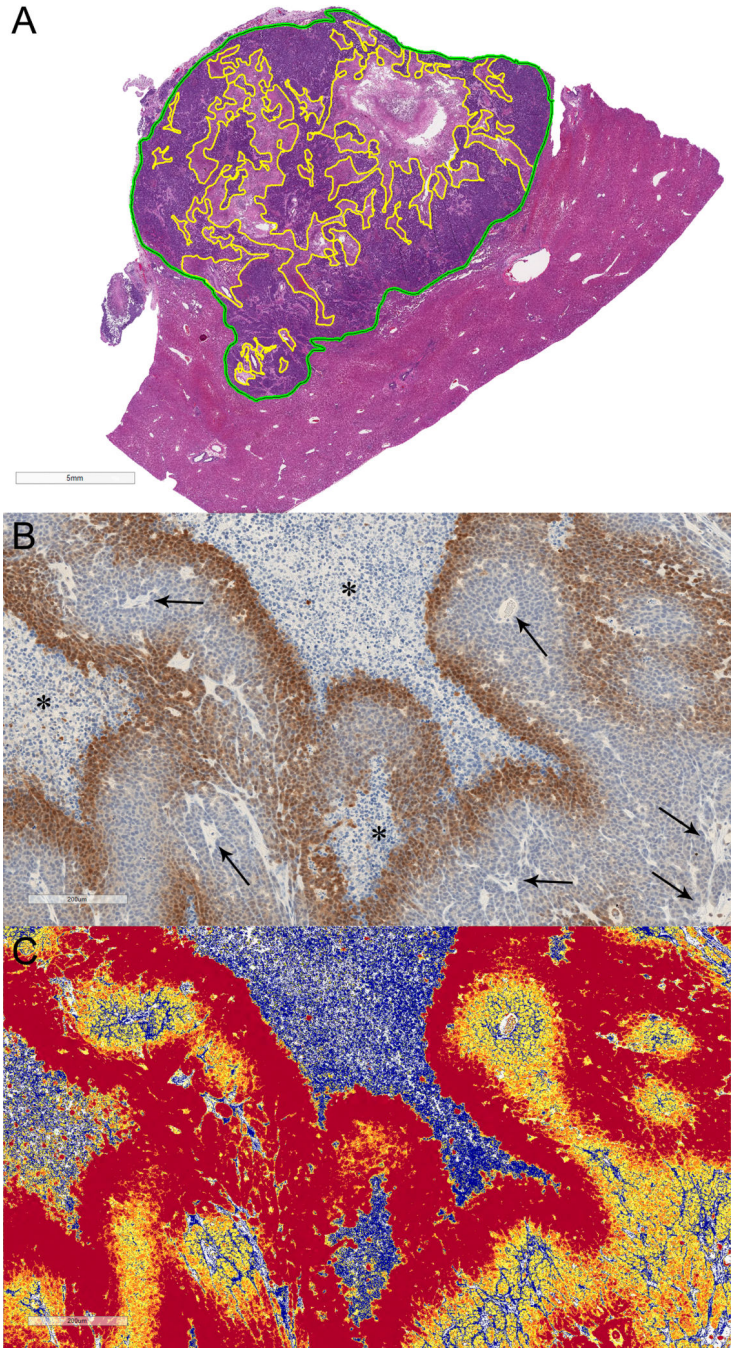

Figure 1.

A) Quantitative histosegmentation technique. Digitized tumor tissue section of a representative VX2 liver tumor. Manually-annotated whole tumor area (green outline) and necrotic areas (yellow outlines) were performed in contiguous tumor slides to obtain the necrotic fraction of the entire tumor. Scale bar = 5 mm. **B)** and **C)** Quantitative color deconvolution technique. **B)** Representative digitized image of tumor hypoxia detected by pimonidazole binding and **C)** corresponding pseudocolor deconvoluted image generated as an algorithm result (colormap). Scale bar = 200 μm. **B)** Dark brown staining outlining tumor

Author Manuscript Author Manuscript Author Manuscript Author Manuscript

necrotic areas (*) represents chronic hypoxia. Numerous tumor vessels are seen throughout the tumor (arrows). **C)** blue pixels = no staining, yellow pixels = weak positive, orange pixels = medium positive, and red pixels= strong positive. Strong positive pixels were considered to quantify each staining, whereas weak and medium positive pixels were assigned to the unstained background.

Author Manuscript Author Manuscript Author Manuscript Author Manuscript

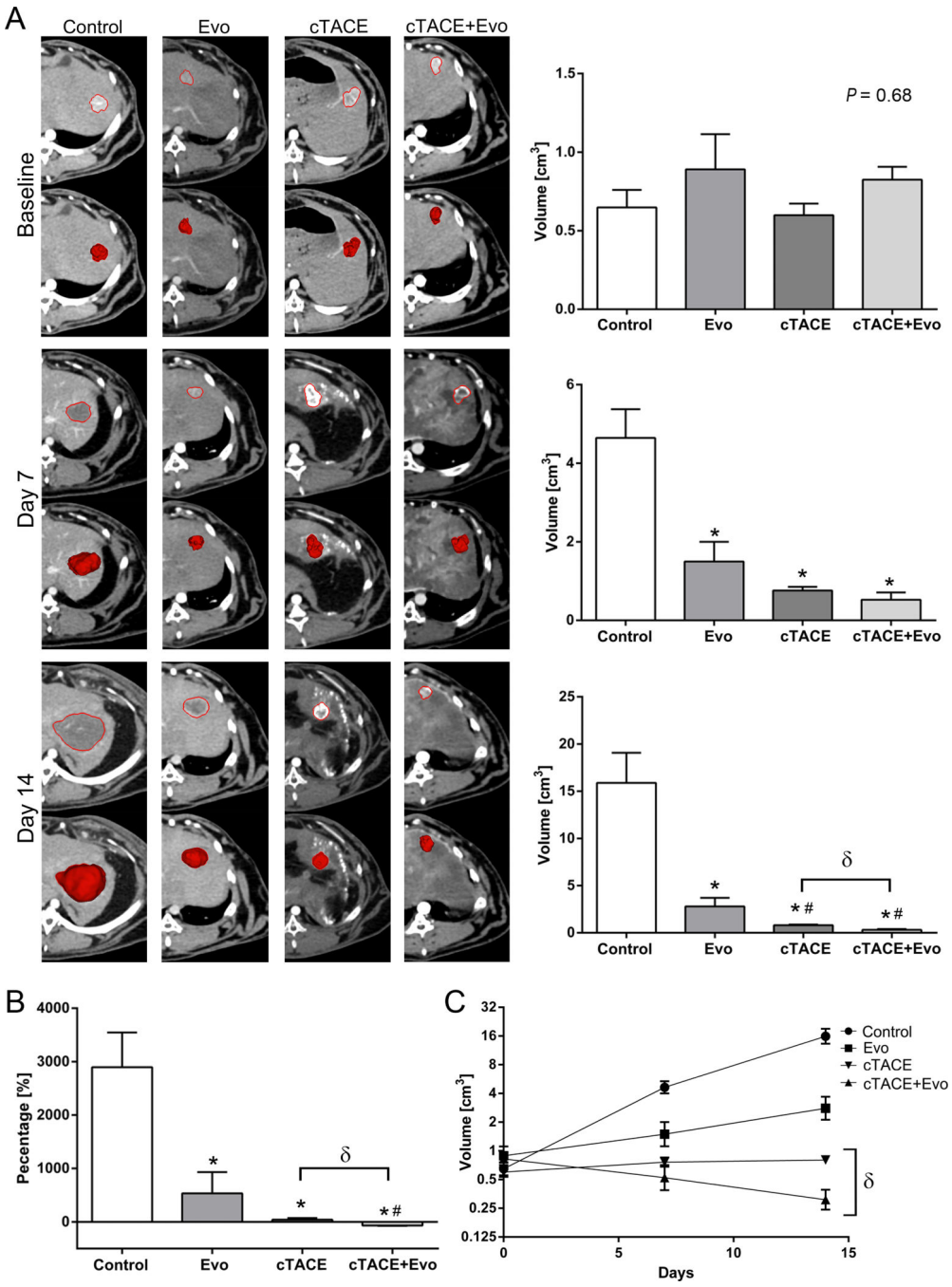

Figure 2.

Quantitative volumetric image analysis at baseline, 7 and 14 days after treatment with Evo (7.7 mg/kg, i.a on day 0), Lipiodol/doxorubicin (0.7 mg/kg, i.a on day 0) based-TACE, Evo (7.7 mg/kg, i.a on day 0) + Lipiodol/doxorubicin (0.7 mg/kg, i.a on day 0) based-TACE. **A)** Representative images of tumor segmentation mask and volume according to the groups (columns) and time points with respective graphs (rows). **B)** Tumor growth rate evaluated at day 14 compared to baseline. **C)** Linear regression analysis to illustrate tumor growth

kinetics. Each bar represents mean ± SEM. * $P < 0.05$ versus control group. # $P < 0.05$ versus Evo group. δ $P < 0.05$ between chemoembolization groups.

Author Manuscript Author Manuscript Author Manuscript Author Manuscript

Author Manuscript Author Manuscript Author Manuscript Author Manuscript

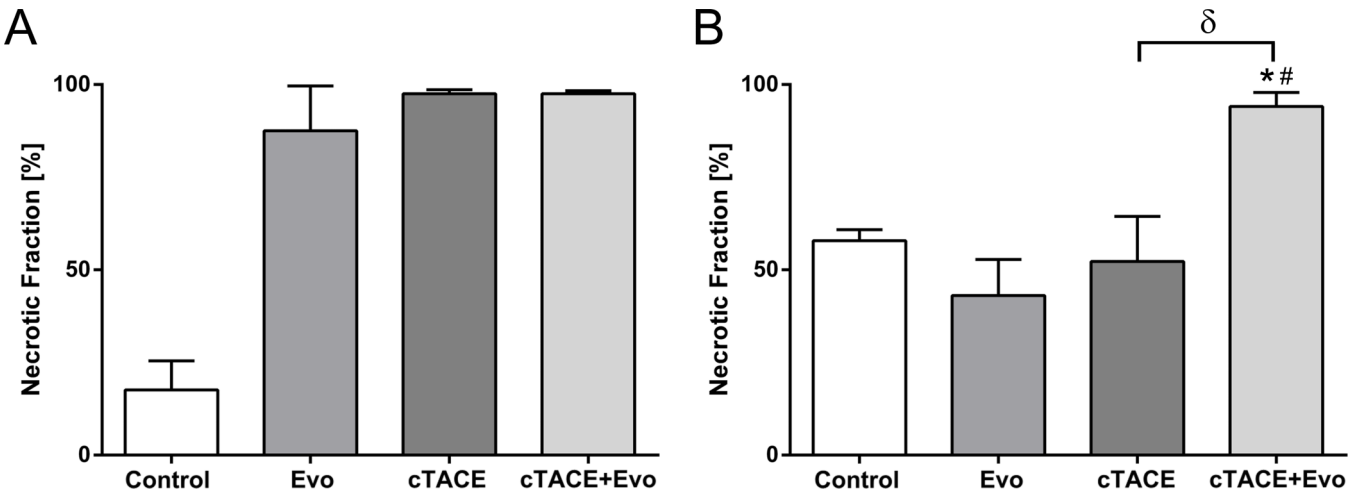

Figure 3.

Quantitative histosegmentation analysis of tumor necrosis at day 2 **(A)** and day 14 **(B)** after treatment. Each bar represents mean ± SEM. * $P < 0.05$ versus control group. $^{\#}$ $P < 0.05$ versus Evo group. $^{\delta}$ $P < 0.05$ between chemoembolization groups.

Author Manuscript Author Manuscript Author Manuscript Author Manuscript

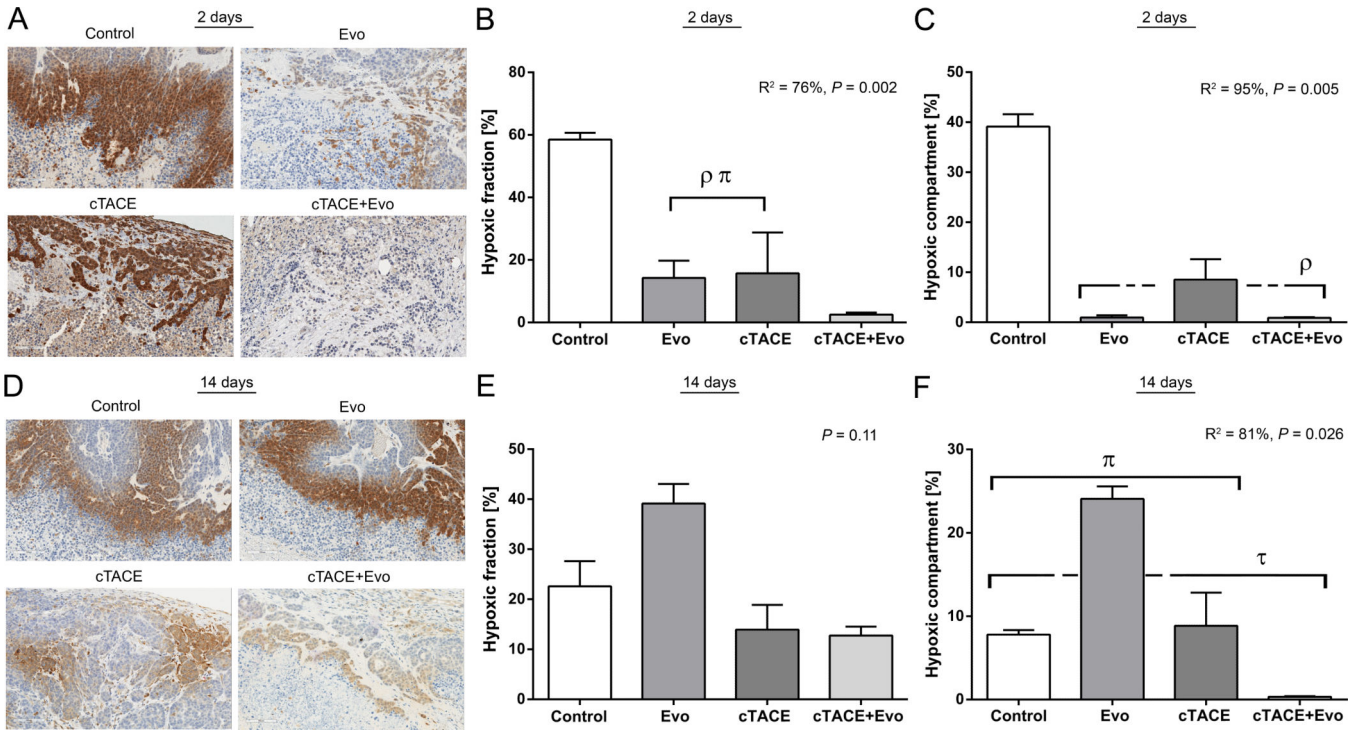

Figure 4.

Quantitative analysis of tumor hypoxia microenvironment changes by pimonidazole staining. **A)** Representative images of tumor hypoxia detected by pimonidazole binding in the 4 study groups at 2 days post selective intraarterial therapy (scale bar = 100 μm). **B)** Percentage of hypoxic fraction (pimonidazole-positive area in the viable tumor) 2 days post treatment. $^{\rho}$ $P < 0.05$ versus control group. $^{\pi}$ $P < 0.05$ versus cTACE+Evo group. **C)** Percentage of the hypoxic compartment (pimonidazole-positive area in the whole tumor area) 2 days post treatment. $^{\rho}$ $P < 0.05$ versus control group. **D)** Representative images of tumor hypoxia detected by pimonidazole binding in the 4 study groups at 14 days post selective intraarterial therapy (scale bar = 100 μm). **E)** Percentage of hypoxic fraction 14 days post treatment. **F)** Percentage of the hypoxic compartment 14 days post treatment. $^{\tau}$ $P < 0.05$ versus Evo group. $^{\pi}$ $P < 0.05$ versus cTACE+Evo group. Each bar represents mean ± SEM.

Author Manuscript Author Manuscript Author Manuscript Author Manuscript

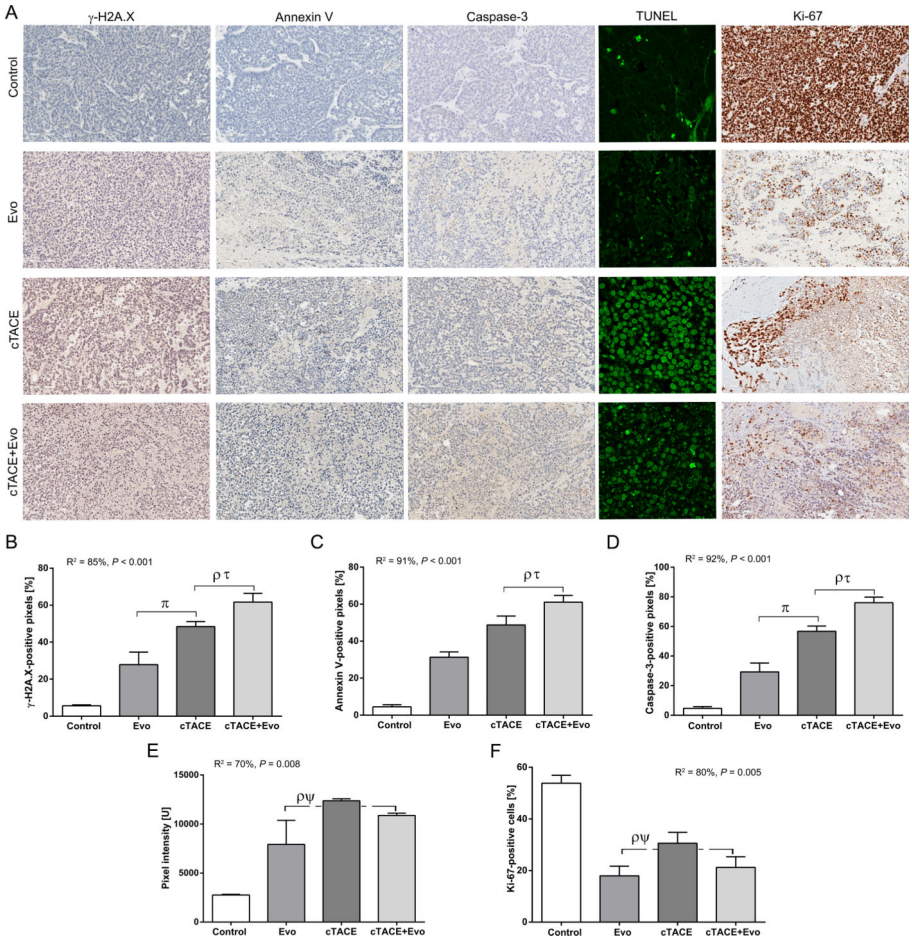

Figure 5.

Quantitative color deconvolution analysis of the expression of biomarkers of DNA damage, apoptosis and cellular proliferation and semi-quantitative analysis apoptosis using terminal deoxynucleotidyl transferase dUTP nick end labeling (TUNEL) performed 2 days post intraarterial interventional treatment. **A)** Representative images of the biomarkers γ-H2A.X, annexin V, caspase-3, Ki-67 at 20x magnification (scale bar = 100 μm) and TUNEL at 40x magnification. **B-F)** Respective biomarkers and TUNEL bar graphs as indicated below corresponding images. Each bar represents mean ± SEM. $^{\rho}$ $P < 0.05$ versus control group. $^{\tau}$ $P < 0.05$ versus Evo group. $^{\pi}$ $P < 0.05$ versus cTACE+Evo group. $^{\Psi}$ $P < 0.05$ versus cTACE group.

Author Manuscript Author Manuscript Author Manuscript Author Manuscript

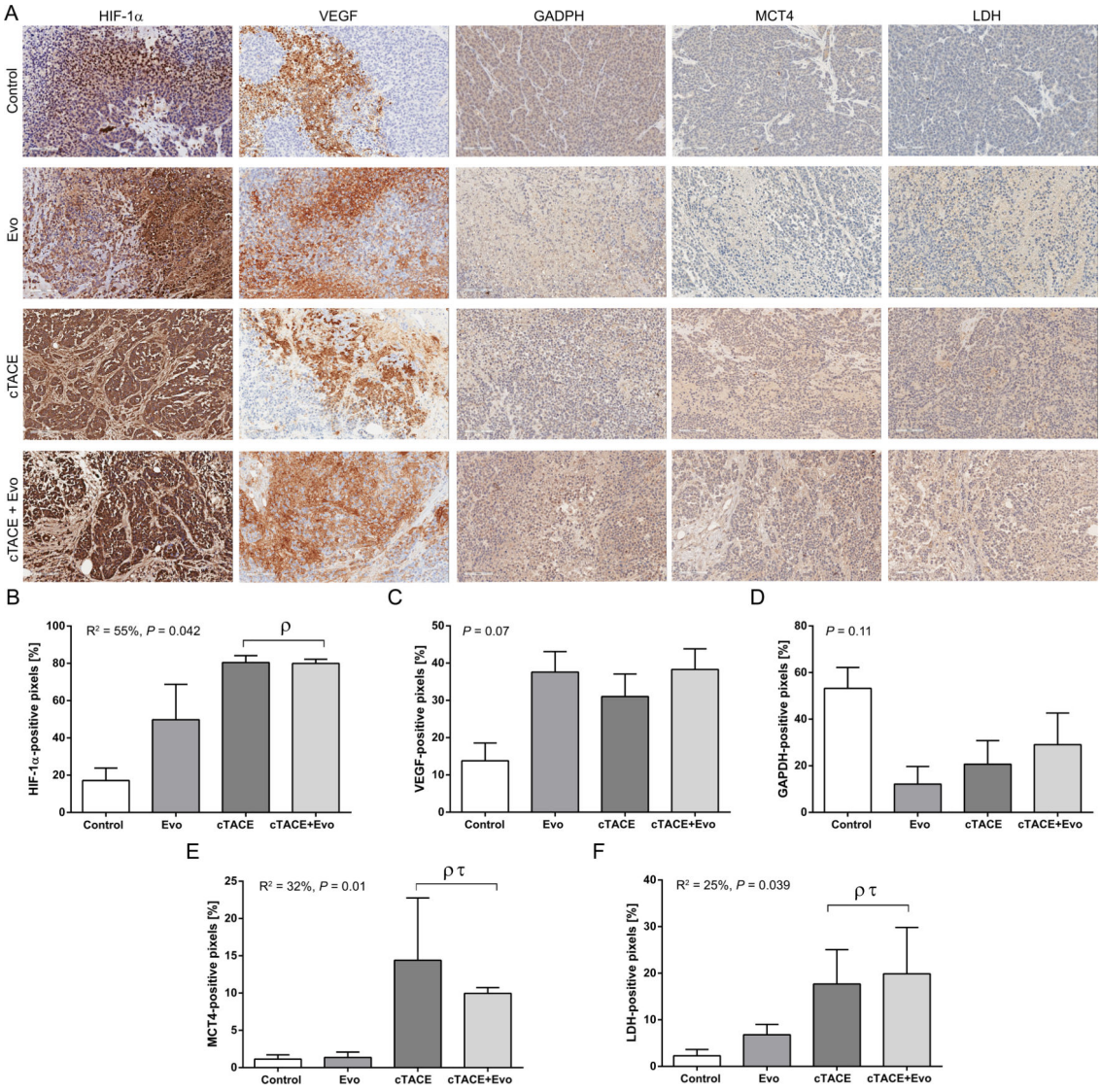

Figure 6.

Quantitative color deconvolution analysis of the expression of endogenous hypoxia and tumor glycolysis biomarkers performed 2 days post intraarterial treatment. **A)** Representative images of the biomarkers HIF-1α, VEGF, GAPDH, MCT4 and LDH at 20x magnification (scale bar = 100 μm). **B-F)** Respective HIF-1α, VEGF and glycolytic biomarkers bar graphs as indicated below corresponding images. Each bar represents mean ± SEM. $^{\rho}$ $P < 0.05$ versus control group. $^{\tau}$ $P < 0.05$ versus Evo group.

Author Manuscript

Author Manuscript

Author Manuscript

Author Manuscript

Table 1

Semi-quantitative evaluation of hepatocellular damage at 14 days post selective intraarterial therapy. The average differences in points of evaluated histological features of cTACE+Evo versus cTACE alone groups are shown.

Histological Features	Difference in points cTACE+Evo vs. cTACE	P-value
Hepatocellular necrosis	1.75	0.248
Vacuolization	−0.5	0.420
Ballooning	0.75	0.420
Lobular inflammation	2.5	0.028
Steatosis	0	1
Biliary hyperplasia	0.5	0.644
Granulation	1.25	0.254
Fibrosis	0	1